

# Parameter Scaling in the Decoherent Quantum-Classical Transition for chaotic rf-SQUIDs

Ting Mao<sup>1</sup> and Yang Yu<sup>1,\*</sup>

<sup>1</sup>*National Laboratory of Solid State Microstructures and Department of Physics, Nanjing University, Nanjing 210093, China*

We numerically investigated the quantum-classical transition in rf-SQUID systems coupled to a dissipative environment. It is found that chaos emerges and the degree of chaos, the maximal Lyapunov exponent  $\lambda_m$ , exhibits non-monotonic behavior as a function of the coupling strength  $D$ . By measuring the proximity of quantum and classical evolution with the uncertainty of dynamics, we show that the uncertainty is a monotonic function of  $\lambda_m/D$ . In addition, the scaling holds in SQUID systems to a relatively smaller  $\hbar_{eff}$ , suggesting the universality for this scaling.

PACS numbers: 05.45.Mt, 03.65.Sq, 03.65.Ta

## I. INTRODUCTION

How classical behavior arises in a quantum mechanical system is one of the essential questions in quantum theory, and has long attracted intense interest. The quantum to classical transition (QCT), which has been well understood to be mainly induced by decoherence caused by the coupling with the environment,<sup>1,2</sup> attains some progresses in recent years. It is proposed that the QCT is controlled by relevant parameters including the effective Planck constant  $\hbar_{eff}$  (i.e., the relative size of the Planck constant), a measure of the coupling with the environment  $D$ , and the Lyapunov exponent  $\lambda$ , for chaotic systems.<sup>3</sup> By computing measures which directly reflect the “distance” between quantum and classical evolutions, it is shown that the distance is controlled by a composite parameter of the form  $\zeta = \hbar^\alpha \lambda^\beta D^\gamma$ . Many efforts on investigating the coefficients  $\alpha$ ,  $\beta$ ,  $\gamma$  have been made<sup>4,5</sup> in different systems such as the kicked harmonic oscillator and the Duffing oscillator. However, in the previous systems,  $\lambda$  is generally a constant. Therefore, the direct illustration of the effect of the Lyapunov exponent  $\lambda$  on the computed distance is still open.

In this article we try to explore the parameter scaling in QCT by using the system of the superconducting quantum interference device (SQUID). Rf-SQUID system has been demonstrated as a well controllable decoherent quantum system. Macroscopic quantum phenomena such as resonant tunneling<sup>6</sup> and level quantization<sup>7</sup> and quantum superposition<sup>8</sup> have been reported. On the other hand, the strong coupling between the SQUID and the environment can introduce chaos. As early as 1983, the chaotic behavior of the SQUID treated as a semi-classical model had been found.<sup>9</sup> Recently, a research shows that a three-junction SQUID can be used to study the dynamics of quantum chaos.<sup>10</sup> Such works motivate us to study the chaotic behavior of SQUID under decoherence induced by environment, which enables us to directly demonstrate the effect of the Lyapunov exponent on QCT.

This article is organized as follows. In Sec.II we numerically investigate the chaotic dynamics of SQUID with coupling to an external environment, and it is shown that the maximal Lyapunov exponent  $\lambda_m$ , which quantifies

the chaotic degree of SQUID, is non-monotonic as a function of  $D$ , a measure of the coupling. Thus we can say in some regimes of  $D$ , the chaos of SQUID is suppressed by the decoherence induced by environment<sup>11</sup>. In Sec.III we use the uncertainty of dynamics as the distance between quantum and classical evolutions, and show that the uncertainty behaves rightly, even in the chaos suppressed region, as a monotonic function of  $\lambda_m/D$ . To the best of our knowledge, this is the first direct demonstration of the scaling relation since it was proposed<sup>3</sup>.

## II. CHAOTIC DYNAMICS OF SQUID

The rf-SQUID system considered here consists of a large superconducting loop interrupted by a single Josephson junction with a critical current  $I_c$ . Under the driving of an external flux  $\phi_{ex}(t)$  with the form of  $\phi_{ex}(0) \cos(\omega_d t)$  (where  $\phi_{ex}(0)$  and  $\omega_d$  respectively denote the driving amplitude and driving frequency), the Hamiltonian for the SQUID system can be given as

$$\hat{H}_D = \frac{\hat{q}^2}{2C} + \frac{(\hat{\phi} - \phi_{ex}(t))^2}{2L} + \frac{I_c \phi_0}{2\pi} \cos(2\pi \hat{\phi} / \phi_0), \quad (1)$$

where  $C$  is the junction capacitance,  $L$  is the rf-SQUID inductance and  $\phi_0 = h/2e$  denotes the superconducting flux quantum. The magnetic flux threading the rf-SQUID  $\hat{\phi}$  and the total charge on the capacitor  $\hat{q}$  are the conjugate variables of the system with the imposed commutation relation  $[\hat{\phi}, \hat{q}] = i\hbar$ .

We can rewrite this Hamiltonian into a dimensionless one<sup>12</sup> as

$$\hat{H}_D = \frac{\hat{Q}^2}{2} + \frac{(\hat{\Phi} - \Phi_{ex}(t))^2}{2} + \frac{I_c}{2\omega_0 e} \cos\left(\frac{2e}{\sqrt{\hbar\omega_0 C}} \hat{\Phi}\right), \quad (2)$$

in which  $\omega_0 = 1/\sqrt{LC}$ ,  $\Phi_{ex}(t) = \sqrt{\frac{\omega_0 C}{\hbar}} \phi_{ex}(t)$ , and  $\hat{Q} = \sqrt{1/\hbar\omega_0 C} \hat{q}$ ,  $\hat{\Phi} = \sqrt{\omega_0 C/\hbar} \hat{\phi}$  satisfy the commutation relation  $[\hat{\Phi}, \hat{Q}] = i$ .

Since no chaos can be seen in the dynamics of isolated quantum systems,<sup>13</sup> to study the chaotic behaviors

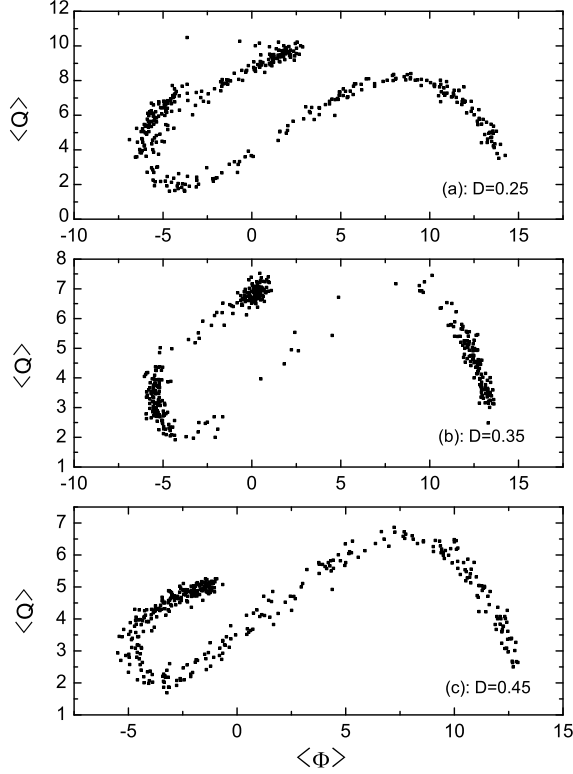


FIG. 1: Poincaré sections for  $D = 0.25, 0.35, 0.45$ , from top to bottom. From middle panel we can see that points are largely confined in three regions, which indicates a non-monotonic transition of chaos.

of the SQUID system, we couple the system to a dissipated environment in the Markovian limit. We adopt the quantum state diffusion (QSD)<sup>14</sup> approach which is widely used in studying open quantum systems<sup>15,16,17</sup> to describe the evolution of this coupled system. The QSD equation for the evolution of the state vector  $|\psi\rangle$  reads

$$|d\psi\rangle = -\frac{i}{\hbar}\hat{H}|\psi\rangle dt + \sum_j \left( \langle \hat{L}_j^\dagger \rangle \hat{L}_j - \frac{1}{2} \hat{L}_j^\dagger \hat{L}_j - \frac{1}{2} \langle \hat{L}_j^\dagger \rangle \langle \hat{L}_j \rangle \right) |\psi\rangle dt + \sum_j (\hat{L}_j - \langle \hat{L}_j \rangle) |\psi\rangle d\xi_j \quad (3)$$

where  $\hat{H}$  is the system Hamiltonian and  $\hat{L}_j$  are the Lindblad operators representing the coupling with the environment.  $d\xi_j$  are independent complex differential Gaussian random variables satisfying  $M(d\xi_j) = M(d\xi_i d\xi_j) = 0$ ,  $M(d\xi_i^* d\xi_j) = \delta_{ij} dt$  (where  $M$  denotes the ensemble mean). For the SQUID system considered here, we have  $\hat{H}$  and  $\hat{L}$  for Equation (3) as  $\hat{H} = \hat{H}_D + \hat{H}_R$ ,  $\hat{L} = \sqrt{D}(\hat{\Phi} + i\hat{Q})$ , where  $\hat{H}_D$  is shown in Equation (2),  $\hat{H}_R = \frac{D}{2}(\hat{\Phi}\hat{Q} + \hat{Q}\hat{\Phi})$ <sup>15,16</sup> is a damping term added to recover the correct equation of motion in the classical limit, and  $D$  is the strength of the coupling with the environment mentioned in the beginning.

Using the powerful QSD library,<sup>18</sup> we numerically

solve the Equation (3) and investigate the change in the dynamics of the SQUID system when increasing the strength of dissipation. A typical set of SQUID parameters is selected here,  $C = 0.1pF$ ,  $L = 300pH$ ,  $I_c = 2.2\mu A$ ,  $\omega_d = 1.14\omega_0$ ,  $\phi_{ex}(0) = 0.2684\phi_0$ , which insures the action of this system is small enough compared with fixed  $\hbar$ .<sup>13</sup> Then we examine 28 different values of  $D$  from slightly dissipated ( $D = 0.23$ ) to heavily dissipated regime ( $D = 1$ ) in our calculation, during which we have the same initial state  $|\psi(t=0)\rangle = |\sqrt{2}(\langle \hat{\Phi} \rangle + i\langle \hat{Q} \rangle)\rangle = (0.877 - 0.566i)$ —the coherent state—and same realization of generating the random numbers. The quantum Poincaré sections, which each comprises of 500 points taken at a fixed phase of the external driving once a driving period, are shown for three representative values of  $D$  in Fig.1(a)-1(c). It can be clearly seen in Fig.1(a) that points forms a uniformly stretched Poincaré profile in the phase space which indicates “chaos” for  $D = 0.25$ . However, for  $D = 0.35$  most of points are confined in three relatively small regions as shown in Fig.1(b), which indicates the suppression of chaos. Then the Poincaré profile similar to the one in Fig.1(a) is recovered in Fig.1(c) when  $D$  is increased to 0.45. Some non-monotonic analogous phenomena have been studied in classical chaotic systems,<sup>11,19</sup> and a qualitative explanation has been proposed there. If the chaotic attractors are narrowly and non-uniformly distributed in phase space, the fluctuation induced by dissipation may cause the neighboring trajectory jump over it, which results in the suppression of chaos. While further increasing dissipation intensity, the structure of the chaotic attractor may be modified and thus spread wider than before. Therefore the system becomes chaotic again. Since  $(\langle \hat{\Phi}(t) \rangle, \langle \hat{Q}(t) \rangle)$  form classical-like trajectories in our calculation, we expect that the explanation is also valid for the suppression of chaos in quantum region.

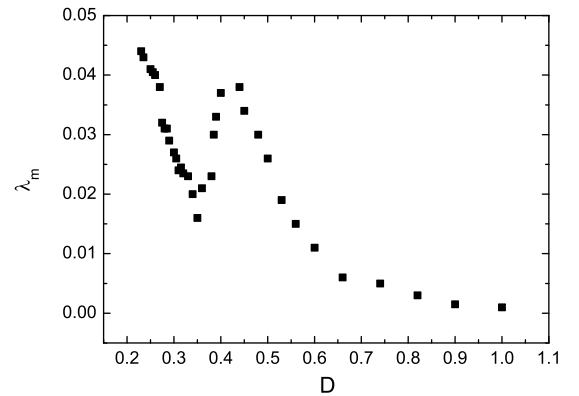


FIG. 2: Maximal Lyapunov exponent  $\lambda_m$  versus  $D$ . The distinctive dip rightly attests the occurrence of suppression of chaos.

To describe this transition of chaos quantitatively, we

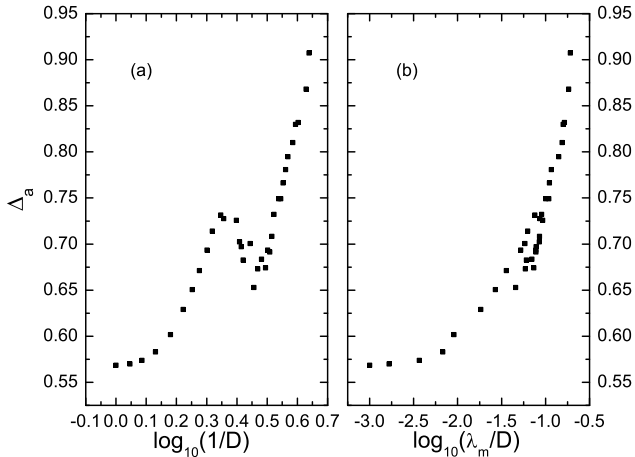


FIG. 3: Averaged uncertainty  $\Delta_a$  as a function of (a)  $D$  and (b) a composite parameter  $\lambda_m/D$ . The monotonic increase of  $\Delta_a$  as a function of  $\lambda_m/D$  in (b) demonstrated the scaling law.

calculate the maximal Lyapunov exponent  $\lambda_m$  for a time series—the expectation value of the magnetic flux  $\langle \hat{\Phi}(t) \rangle$ —at each value of  $D$ . The calculation is based on the method and programs<sup>20,21</sup> which are specifically designed for the analysis of nonlinear time series. With carefully chosen parameters as the delay time  $d = 3$ , the embedding dimension  $m = 3$  and the scaling length  $s = 1.4\%$  for the calculation to best meet the requirements in Ref.18, the sufficient convergency of the Lyapunov exponent is guaranteed. The result is shown in Fig.2, in which the graph of  $\lambda_m$  versus  $D$  has a distinctive dip in a approximate region of  $D = 0.25 \sim 0.45$ , indicating the suppression of chaos. We also repeat the whole calculation above in some different realization of random numbers with the SQUID parameters and the initial state fixed, and find the curves are quite analogous to the one in Fig.2.

### III. EFFECT OF MAXIMAL LYAPUNOV EXPONENT ON QCT

With the non-monotonic relationship between maximal Lyapunov exponent  $\lambda_m$  and the strength of the coupling with the environment  $D$ , we can directly investigate the effect of  $\lambda_m$  on QCT. To measure the “distance” between quantum and classical evolution, we use the well known quantity—the uncertainty of dynamics

$\Delta = \sqrt{\langle (\hat{\Phi} - \langle \hat{\Phi} \rangle)^2 \rangle} \sqrt{\langle (\hat{Q} - \langle \hat{Q} \rangle)^2 \rangle}$ , which is simple for calculation and adequate to describe the QCT. According to the commutation relation  $[\hat{\Phi}, \hat{Q}] = i$ , it follows that  $\Delta \geq 0.5$ . By solving Equation (3) with same calculating parameters as in Sec.II, we get a time series of the uncertainty  $\Delta(t)$  at each value of  $D$ . After averaging each series of  $\Delta(t)$  over a reasonably long time ( $> 100$

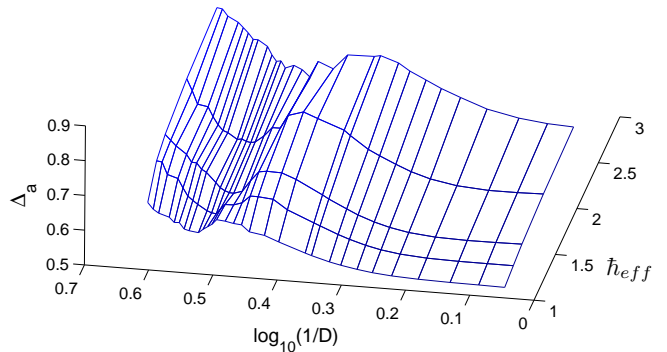


FIG. 4: (Color online) Averaged uncertainty  $\Delta_a$  as a function of  $D$  and  $\hbar_{eff}$ . The parameters for the system with largest effective Planck constant  $\hbar_{eff} = 2.6$  has been shown in text. Other  $\hbar_{eff}$  and corresponding sets of parameters are listed in Table.I.

TABLE I:  $\hbar_{eff}$  and corresponding parameters

| $\hbar_{eff}$ | $I_c(\mu A)$ | $L(pH)$ | $C(pF)$ | $\omega_d(\omega_0)$ | $\phi_{ex}(0)(\phi_0)$ |
|---------------|--------------|---------|---------|----------------------|------------------------|
| 1             | 4.6          | 100     | 3.95    | 0.65                 | 0.081                  |
| 1.2           | 3.35         | 150     | 2.16    | 0.71                 | 0.1041                 |
| 1.4           | 2.67         | 200     | 1.29    | 0.78                 | 0.1273                 |
| 1.9           | 2.46         | 250     | 0.36    | 0.99                 | 0.1851                 |

periods of the external driving), we obtained the curve of the averaged uncertainty  $\Delta_a$  versus  $D$  and showed in Fig.3(a), where  $D$  has the same sequence of values as in Fig.2. It can be clearly seen that in Fig.3(a) a obvious dip emerges in the very regime where chaos is suppressed by the dissipation, which implies QCT directly depends on the degree of chaos. Motivated by this, we combine  $\lambda_m$  and  $D$  with the form of  $\lambda_m/D$  which is inferred in Ref.2 and look into the relationship between  $\Delta_a$  and such composite single parameter. Shown Fig.3(b) is an example of  $\Delta_a$  vs.  $\lambda_m/D$ . One can find that the dip is rubbed out and  $\Delta_a$  approximately shows a monotonic increasing in  $\lambda_m/D$  with two distinct regimes of small and large increasing rates.<sup>3</sup> Therefore we demonstrate the scaling between  $\lambda_m$  and  $D$  holds over a considerable range in  $\Delta_a$ . It is noticed that the points which lie in the dip in Fig.3(a) spread slightly around the curve in Fig.3(b). We conjecture this spread could be mainly attributed to the calculating error<sup>20</sup> of  $\lambda_m$  which is induced by the inevitable quantum noise added into the trajectory of  $(\langle \hat{\Phi}(t) \rangle, \langle \hat{Q}(t) \rangle)$ , especially when chaos is suppressed and the value of  $\lambda_m$  is comparatively small.

Now we examine this scaling law for the SQUID system with a smaller effective Planck constant  $\hbar_{eff}$ . To obtain a smaller  $\hbar_{eff}$ , it is not straightforward for the SQUID system to directly manipulate the value of  $\hbar$ .<sup>12</sup> Instead, we enlarge the action of the SQUID system simply by changing parameters in the Hamiltonian; the larger the

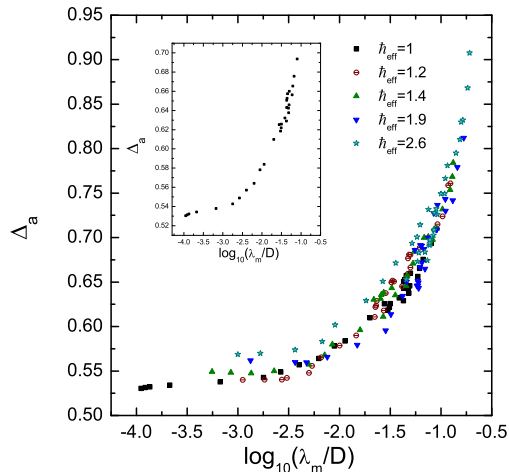


FIG. 5: (Color online)  $\Delta_a$  versus a composite parameter  $\lambda_m/D$  for different effective Planck constant. It is shown that the scaling law holds for systems with different  $\hbar_{eff}$ . Inset: The curve with  $\hbar_{eff} = 1$  is shown separately.

action the smaller  $\hbar_{eff}$ , and vice versa.<sup>13</sup> By deliberately selecting the set of parameters including  $I_c$ ,  $L$ ,  $C$ ,  $\omega_d$  and  $\phi_{ex}(0)$ , we can enlarge the action and maintain the chaotic dynamics of the system at the same time. The values of these parameters are not difficult to modulate for a realistic SQUID system where  $I_c$  could become controllable by replacing the single Josephson junction with a small loop (dc SQUID) which contains two identical Josephson junctions,<sup>6</sup>  $C$  and  $L$  are both under the upper realistic limit of typical Josephson junctions. We select four sets of parameters for the SQUID systems each of which has a smaller  $\hbar_{eff}$  compared with the foregoing system's. Assuming the smallest  $\hbar_{eff}$  is equal to 1 and comparing the actions of the systems which are measured with the system size,<sup>13</sup> we approximately gain the value of other effective Planck constants as follow, 1.2, 1.4, 1.9, 2.6, where 2.6 is the value of the foregoing system's  $\hbar_{eff}$ . Then we apply the same calculating procedures to these systems, and the results are shown in Fig.4 and Fig.5 which also include the data of the foregoing system for

comparison. Fig.4 shows the averaged uncertainty  $\Delta_a$  as a function of  $D$ ,  $\hbar_{eff}$ . For each  $\hbar_{eff}$ , a distinct dip exists as expected in the region where chaos is suppressed by the dissipation of environment. Fig.5 shows the same data plotted as a function of  $\lambda_m/D$ , in which, the behavior of  $\Delta_a$  for each  $\hbar_{eff}$  is considerably the same, which demonstrates the scaling between  $\lambda_m$  and  $D$  is still valid for a system with relatively small  $\hbar_{eff}$ . For clarity, we separately show the curve with  $\hbar_{eff} = 1$  in the inset of Fig.5. Since a larger action is helpful to undermine the effect of quantum noise, more accurate  $\lambda_m$  can be gained for the system with smaller  $\hbar_{eff}$ , which, is reflected in the lack of noticeable spread around the curve in the inset.

We also chose some different random numbers generator to repeat the calculation for SQUID systems with different  $\hbar_{eff}$ , and succeed in getting same qualitative conclusions as discussed above.

#### IV. CONCLUSION

In summary, we investigated QCT in chaotic rf-SQUIDs. The suppression of chaos induced by environment dissipation was observed in quantum regime. It is found that the quantum to classical transition in the presence of a dissipated environment is governed by a composite parameter  $\lambda_m/D$ . It could be expected the scaling law between  $\lambda_m$  and  $D$  would holds over a wide range of  $\hbar_{eff}$ . However, to generalize this scaling to the one involving  $\hbar_{eff}$ ,  $\lambda_m$  and  $D$  and to reveal the coefficients between them are still open questions needed to explore.

#### V. ACKNOWLEDGMENTS

This work was partially supported by the NSFC (under Contract Nos. 10674062,10725415), the State Key Program for Basic Research of China (under Contract Nos. 2006CB921801), and the Doctoral Funds of the Ministry of Education of the People's Republic of China (under Contract No. 20060284022).

\* Electronic address: yuyang@nju.edu.cn

<sup>1</sup> W. H. Zurek, Rev. Mod. Phys **75**, 715 (2003).

<sup>2</sup> The presence of classical chaos may lead to novel quantum phenomena in some quantum systems isolated from the environment. These phenomena are out of scope of our discussion in this paper.

<sup>3</sup> A. K. Pattanayak, B. Sundaram, and B. D. Greenbaum, Phys. Rev. Lett **90**, 014103 (2003).

<sup>4</sup> F. Toscano, R. L. de Matos Filho, and L. Davidovich, Phys. Rev. A **71**, 010101 (2005).

<sup>5</sup> A. Gammal, and A. K. Pattanayak, Phys. Rev. E **75**, 036221 (2007).

<sup>6</sup> R. Rouse, S. Han, and J. E. Lukens, Phys. Rev. Lett **75**, 1614 (1995).

<sup>7</sup> P. Silvestrini, V. G. Palmieri, B. Ruggiero, and M. Russo, Phys. Rev. Lett **79**, 3046 (1997).

<sup>8</sup> J. R. Friedman, V. Patel, W. Chen, S. K. Tolpygo, and J. E. Lukens, Nature (London) **406**, 43 (2000); C. H. van der Wal, A. C. J. ter Haar, F. K. Wilhelm, R. N. Schouten, C. J. P. M. Harmans, T. P. Orlando, S.Lloyd, and J. E. Mooij, Science **290**, 773 (2000).

<sup>9</sup> K. Fesser, A. R. Bishop and P. Kumar, Appl. Phys. Lett **43**, 123 (1983).

<sup>10</sup> E. N. Pozzo, and D. Domínguez, Phys. Rev. Lett **98**,

- 057006 (2007).
- <sup>11</sup> H. Yamazaki, T. Yamada, and S. Kai, Phys. Rev. Lett **81**, 4112 (1998).
- <sup>12</sup> M. J. Everitt, New. J. Phys **11**, 013014 (2009).
- <sup>13</sup> S. Habib, K. Jacobs, and K. Shizume, Phys. Rev. Lett **96**, 010403 (2006).
- <sup>14</sup> I. C. Percival, *Quantum State Diffusion* (Cambridge University Press, Cambridge, England, 1998).
- <sup>15</sup> T. A. Brun, I. C. Percival, and R. Schack, J. Phys. A **29**, 2077 (1996).
- <sup>16</sup> A. Kapulkin, and A. K. Pattanayak, Phys. Rev. Lett **101**, 074101 (2008).
- <sup>17</sup> Y. Ota, and I. Ohba, Phys. Rev. E **71**, 015201 (2005).
- <sup>18</sup> R. Schack, T. A. Brun, and I. C. percival, J. Phys. A **28**, 5401 (1995); R. Schack, T. A. Brun, Comput. Phys. Commun. **102**, 210 (1997).
- <sup>19</sup> K. Matsumoto, and I. Tsuda, J. Stat. Phys. **31**, 87 (1983).
- <sup>20</sup> H. Kantz, Phys. Lett. A **185**, 77 (1994).
- <sup>21</sup> R. Hegger, H. Kantz, and T. Schreiber, Chaos **9**, 413 (1999).